KAOLINITE WETTABILITY – THE EFFECT OF SALINITY, pH AND CALCIUM

Evgenia V. Lebedeva, Andrew Fogden, Tim J. Senden, Mark A. Knackstedt
Dept of Applied Mathematics, Australian National University, Canberra, Australia

This paper was prepared for presentation at the International Symposium of the Society of Core Analysts held in Halifax, Nova Scotia, Canada, 4-7 October, 2010

ABSTRACT

A method is developed to prepare smooth, thin coats of kaolinite particles on a substrate, so that the particles remain immobilized in contact with crude oils, brines and cleaning liquids. The coated substrates are used for determining contact angle of crude oil drops in brine and analyzing deposition of wettability-altering oil components after longer-time aging, in both cases for a matrix of sodium chloride brines with varying concentration, pH and presence of calcium. The hysteresis in contact angle from receding to advancing, indicative of shorter-time adhesion of oil to kaolinite, increases with decrease in sodium chloride concentration and/or decrease in pH. The adhesion map is qualitatively similar to those in the literature for mica and glass. At natural pH, all brines containing sodium and calcium chlorides with total ionic strength above 0.1M give low adhesion, while all above this cut-off give higher adhesion, especially for calcium chloride in isolation. After longer-time aging, all kaolinite substrates bear some oil deposit, with asphaltene-based deposition generally decreasing with ionic strength and correlating with the drop adhesion results. From high-resolution SEM imaging, high sodium chloride limits deposition to kaolinite edges, while high calcium chloride reduces oil penetration into kaolinite aggregates. X-ray micro-CT analysis of a kaolinite-rich sandstone verifies that no mass movement of large plates occurs during brine flooding at high or low salinity.

INTRODUCTION

Kaolinite is one of the most abundant types of clay in reservoir rocks, and significantly influences reservoir wettability and pore distribution of oil and brine. This applies to both the initial state established in the formation brine by aging, and its subsequent evolution as oil and brine redistribute by flooding in secondary or tertiary recovery. Macroscopic core floods often point to kaolinite increasing oil-wetness indices, and microscopy of plugs, e.g. using cryo-SEM [1], often show oil filling kaolinite aggregates, the particle surfaces of which are presumably rendered oil-wet. Such microscopic studies are difficult to generalize, as observations depend strongly on kaolinite configurations, whether pore-lining or -filling, other mineral components present, and local saturation histories. Further, measures of local wettability in rock, such as oil-brine contact angles or presence of adsorbed or deposited asphaltenes and resins, are difficult to assign or even access.

For this reason, smooth monomineralic substrates such as quartz [2] or mica [3] were used to measure intrinsic wettability without the capillary effects of pore confinement,

and for simple saturation histories of the crude-oil brine combination. Contact angle is typically measured a) directly but without aging, for crude oil against a brine-immersed substrate [2-4], or b) indirectly but with aging, by conditioning the brine-lined substrate in crude oil, then flushing excess oil and measuring alkane-water contact angle on the deposit-bearing substrate [2-3]. For simple brines containing only sodium chloride, some general trends have emerged. Almost all crude oil-model (alumino)silicate combinations exhibit high contact angle hysteresis and oil adhesion at low salinity and pH and low hysteresis and non-adhesion for high salinity and pH [2-4]. Brines with divalent ions are less often studied systematically, as results are more crude oil-specific [3]. The goal of the current study was to cast kaolinite in the form a suitable model substrate and extend these wettability studies, both without and with aging, to this highly relevant mineral.

The importance of kaolinite has further increased in recent years with the accumulating weight of empirical evidence implicating kaolinite in enhancement of oil recovery by low salinity flooding. Early studies in sandstones were interpreted in terms of mobilization of kaolinite fines [5], while later flooding experiments and trials, in which fines production in the effluent was generally not observed, concluded that kaolinite wettability was altered towards water-wetness by ion exchange [6]. The mechanism(s) are still not fully resolved, with responses being highly dependent on rock, oil and brine compositions, and initial wettability state [7-8]. Although the current study is limited to single brines, without change from formation to injected or tertiary injected brines, it aims to establish base cases for future assessment of the effect of such switches.

EXPERIMENTAL

Oil, Brines and Preparation of Kaolinite-Coated Substrates

The crude oil, from the Minnelusa formation (Gibbs Field, Wyoming), has density 0.9062 gcm^{-3}, viscosity 77.2 mPa.s, n-C_7 asphaltene content 9.0 wt%, and acid and base numbers 0.17 and 2.29 mg KOH/g oil (all at 25 ^oC) [9]. The oil was filtered and centrifuged before use. The 24 brines in columns 1-3 of Table 1 were prepared using analytical grade NaCl and $CaCl_2.2H_2O$ and deionized water from a Millipore Milli-Q system, then vacuum degassed for 15 min. The brines at unadjusted, natural pH (denoted "n") were of pH 5.7 ± 0.4, while the acidic and basic brines were adjusted using HCl and NaOH, then again degassed for 10 min., to pH 4.0 ± 0.1 and 9.0 ± 0.2, respectively. Well-crystallized kaolinite KGa-1b (Washington County, Georgia; Clay Minerals Society Source Clay Repository) [10-11] was used without further cleaning. A stable, aqueous, fine-particle suspension was prepared without chemicals, by repeated steps of stirring, sonication, adjustment to pH 9.8, centrifugation and decanting, and final heating in an open beaker to a solids concentration of 7 wt%. Around 0.05 g of suspension was pipetted as several drops onto each pre-cleaned microscope glass slide (76x25 mm^2), and thinly spread over the majority of its area. A heat gun (T ~120 ^oC) was then swept in one direction over the wet coat to rapidly immobilize its particles. Each coated slide was flushed under running tap water to remove the occasional loosely bound particle, and then dried with N_2.

Table 1. Average and standard deviation of contact angle hysteresis and asphaltene deposition after aging, on kaolinite-coated substrates, for varying brine pH and concentrations of sodium and calcium chlorides.

pH	[NaCl], M	[$CaCl_2$], M	Hysteresis, degrees	Deposition, GSV
n	0	0	35 ± 13	25.6 ± 2.8
n	0.01	0	36 ± 24	21.7 ± 5.0
n	0.1	0	24 ± 6	24.0 ± 2.6
n	1	0	9 ± 11	14.0 ± 7.2
n	0	0.001	57 ± 23	26.7 ± 3.0
n	0	0.01	60 ± 3	11.9 ± 1.9
n	0.01	0.01	20 ± 7	21.1 ± 4.3
n	0.1	0.01	8 ± 3	17.4 ± 2.2
n	1	0.01	2 ± 4	13.3 ± 5.6
n	0	0.1	13 ± 10	11.2 ± 4.5
n	0.01	0.1	9 ± 12	18.5 ± 1.7
n	0.1	0.1	17 ± 15	15.1 ± 2.9
n	1	0.1	1 ± 4	17.2 ± 2.8
n	0.01	1	16 ± 9	8.4 ± 2.2
n	0.1	1	2 ± 2	11.8 ± 6.6
n	1	1	9 ± 5	11.9 ± 5.1
4	0	0	88 ± 3	22.8 ± 4.2
4	0.01	0	66 ± 17	21.8 ± 2.4
4	0.1	0	46 ± 23	20.9 ± 5.0
4	1	0	13 ± 8	13.8 ± 6.5
9	0	0	12 ± 3	18.6 ± 2.3
9	0.01	0	32 ± 8	7.4 ± 3.2
9	0.1	0	28 ± 8	26.9 ± 2.8
9	1	0	7 ± 8	25.6 ± 3.3

Contact Angle Measurements

Captive pendant drop measurements of receding and advancing angle were performed at 23-24 ^{o}C with a contact angle goniometer (KSV Instruments), using a rectangular fluid cell. A piece of kaolinite-coated glass, ~1x1 cm^2, was mounted on a chuck, immersed in the brine-filled fluid cell and equilibrated for 1 h., then affixed to the cell lid with coated side facing down. A crude oil drop was pumped out upwards at 0.8 μl/s from a stainless steel hooked syringe of outer and inner diameter 0.65 and 0.31 mm, and left for 10 min. at the syringe tip to equilibrate with the brine. The drop was then contacted with the kaolinite layer and grown slightly more (to a volume ~4 μl), directly after which the drop profile was imaged and its receding contact angle was measured through the brine. The drop was left for 30 min. in this state to give the oil the opportunity to partially adhere to kaolinite. It was then retracted at the same rate and the brine-advancing contact angle was similarly measured. The procedure was then duplicated for a second drop on a clean area.

Preparation of Oil-Aged Substrates

For each brine, 4 glass vials were filled with 3.0 ml of it, into which a kaolinite-coated glass piece (~7.5x25 mm^2) was immersed, followed by light vacuum degassing for 10

min. The sealed vials with their sample piece were equilibrated at 60 ^{o}C for 2 days, or only 20 h. for the basic brines (after which their pH was 8.3 ± 0.6) to avoid further acidification by re-absorption of CO_2. Each piece was removed with tweezers and, in this brine-saturated state, immediately immersed (< 2 s transfer time) in 2.0 ml of crude oil, preheated to 60 ^{o}C, in a glass vial. The sealed vials were aged at 60 ^{o}C for 8 days, after which each piece was directly transferred to its own 2.5 ml bath of decalin to dissolve the majority of the adhering bulk oil, then after 1 h. to a second such decalin-filled vial for 40 h. of further soaking. This was followed by transfer to a 2.5 ml heptane-filled vial for 10 days to remove maltene residues, then to 2.5 ml of 77.5/22.5 (v/v) methanol/water for 50 min. to dissolve salt, after which each piece was removed to dry ambiently. The uncoated backside of each slide was wiped with water-wetted tissue to remove any oil deposits.

Measurements of Oil-Aged Substrates

As asphaltene-based residues on the brine/oil-treated kaolinite-coated pieces produce a brownish tinge, a document scanner (Konica Minolta C252) provided a simple, rapid means to compare the extent of deposition over this large data set. All 96 pieces, plus untreated control pieces, were imaged simultaneously with coated side facing the glass. From the 300 dpi jpeg scanned image, the statistics of their 8-bit grayscale values (GSV) were extracted using ImageJ software. Of the 4 pieces for each brine, that with deposition closest to the average was analyzed by microscopy. Half of this piece was lightly sputter coated with platinum and imaged with a field emission scanning electron microscope (FESEM, Zeiss UltraPlus Analytical) under high vacuum in secondary electron mode at 1 kV. The other half was imaged as-is using an atomic force microscope (AFM, Nanoscope III, Digital Instruments), scanning with high sensitivity Super A scanner at 0.89 Hz in tapping mode. Similar analyses were performed on untreated kaolinite-coated pieces.

X-ray μ-CT of Rock Plug

A sandstone with permeability 200 mD, total porosity 10 %, total fraction of clay 3.2 %, porosity associated with clay 9.4 %, and with kaolinite as the dominant clay type, was cored to a 5 mm diameter plug. The ANU μ-CT facility [12] was used to 3D image the plug in 4 states, in each case acquiring 2880 projections of 2048^2 pixels, with pixel size ~3 μm, using filtered Bremsstrahlung with the x-ray source set to 80 kV and 110 μA. The plug was first imaged dry, then heat shrunk and lightly vacuum saturated with 0.1M $CaCl_2$ and imaged, then flooded under atmospheric pressure for 2 h. with 0.001M $CaCl_2$ and imaged, then similarly flooded with deionized water and imaged. Projections were reconstructed and the 4 tomograms were superposed using a registration algorithm [13].

RESULTS AND DISCUSSION

Structure of Kaolinite-Coated Substrates

The above-mentioned procedure results in a smooth, only slightly opaque, uniform coat of thickness just over 1 μm. Figure 1 gives representative high-resolution FESEM and AFM surface images, showing platy, fine kaolinite as single particles or stacks of several of these, often with larger plates overlain with smaller plate fragments. Although plate

orientation is mainly parallel to the substrate, many are tilted (most apparent from AFM), and inter-particle pore throats are typically < 100 nm. Our approach attains much lower thickness than other literature methods [11], without sacrificing uniform coverage, by combining a high quality suspension and rapid immobilization post-application. The thin coats thus serve to maximize smoothness and particle stability to aid in probing the true oil adhesion and deposition via contact angle measurements and aging.

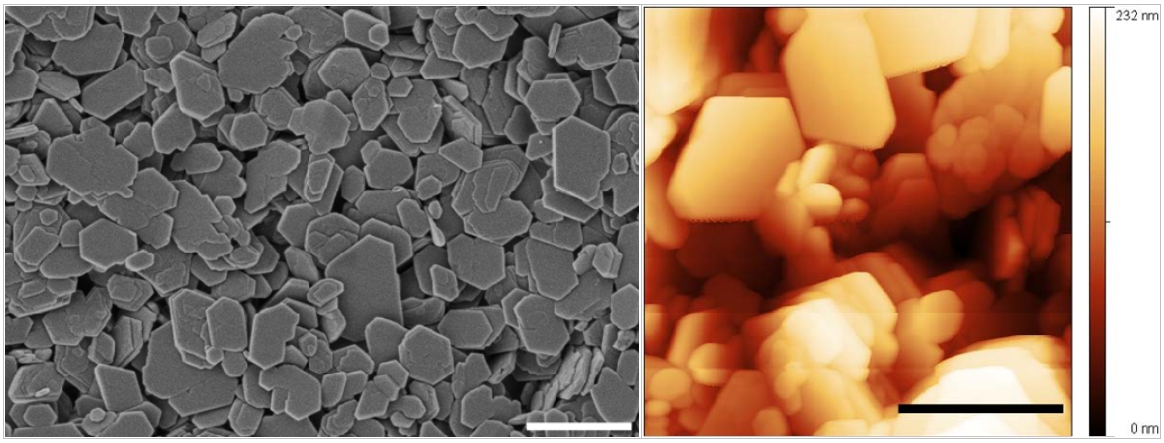

Figure 1. Left: FESEM image, and right: AFM height image, of kaolinite coats. Scale bars are 500 nm.

Oil-Kaolinite Adhesion

Over all 24 brines analyzed, the brine-receding contact angle from crude oil drop growth on the kaolinite-coated substrate varies little, with average and standard deviation of 35.4 ± 5.4^{o}. The brine-advancing angle after brief aging and drop retraction is always greater, and its increase from receding to advancing, is termed the contact angle hysteresis. The average and standard deviation of angle hysteresis from the replicate experiments for each brine are listed in Table 1. The trends are shown in the 3D graphs of Figs. 2a and b for the 4 NaCl concentrations (0, 0.01, 0.1 and 1M) at either the a) 3 pH values (4, natural and 9), or b) 3 concentrations (0.01, 0.1 and 1M) of added $CaCl_2$. Oil drop retraction results in 3 possible states: bulk oil remains adhered due to snap-off (adhesion), or only small droplets remain (transition), or removal is clean and complete (non-adhesion) [2-3]. This categorization of our observations agrees with measured angle hysteresis: the average over all brines displaying adhesion, transition and non-adhesion is 63.5^{o}, 19.8^{o} and 11.5^{o}. Thus increased hysteresis can be regarded as increased oil-kaolinite adhesion.

In Fig. 2a, angle hysteresis at pH 4 increases strongly as NaCl concentration decreases from 1M. This trend is also present at the natural pH and pH 9, although weaker and reaching a plateau around 0.01 and 0.1M, respectively, and actually decreasing below 0.01M for the latter. Accordingly, the increase in hysteresis with decreasing pH becomes progressively stronger as salinity is reduced. This strong adhesion to kaolinite at low pH and NaCl concentration, and non-adhesion at the opposite extreme of high pH and salinity, is shared by the vast majority of crude oil-silicate substrates in the literature [2-4]. The precise location of the boundary and transition between these states is, though,

specific to the system. Adhesion maps versus NaCl concentration and pH for a similar crude (Prudhoe Bay A-93) on mica [3] give a boundary close to that for our Minnelusa oil/kaolinite system, while A-93/glass [2] shows stronger, more widespread adhesion. For all sodium and/or calcium chloride brines at natural pH in Fig. 2b and Table 1, adhesion only occurs at low concentrations (0.001-0.01M) of $CaCl_2$ in isolation. The decrease in adhesion with salinity in Fig. 2a extends to the mixed-salt brines in Fig. 2b. At natural pH, all brines with total ionic strength above 0.1M give hysteresis less than 17°, while all compositions above this strength exhibit hysteresis greater than 20°.

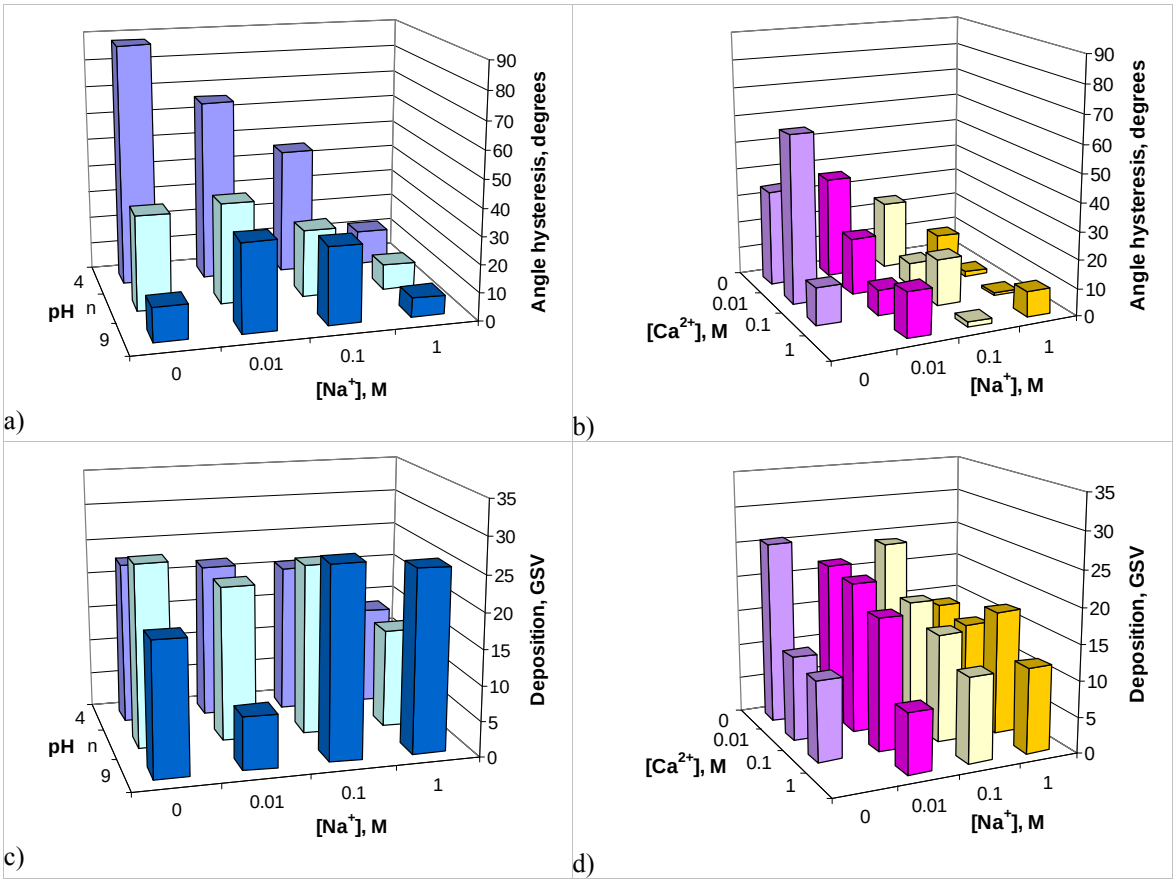

Figure 2. a-b) Average contact angle hysteresis for a crude oil drop in brine, and c-d) average extent of asphaltene deposition after aging, on kaolinite-coated substrates, as a function of NaCl concentration and a) and c): pH, with "n" denoting its natural value, or b) and d) concentration of added $CaCl_2$ at pH n.

For the low salinity NaCl brine at pH 4, below the isoelectric point (IEP) for Minnelusa crude [14], the polar components of the oil will be protonated at its brine interface [4], while kaolinite, with an overall IEP at pH 2-3, will be net negatively charged. The quite long-ranged DLVO electrostatic attraction, together with van der Waals attraction, will rupture the brine thin film and oil will adhere to the kaolinite. Rise in brine acidity to natural pH and pH 9 switches the charge on both interfaces to more negative, switching their electrostatics towards repulsion, so reducing adhesion as in Fig. 2a. Increase in NaCl

concentration decreases the range of electrostatics, reducing the attraction and adhesion at pH 4, again in line with Fig. 2a. However, decreasing adhesion with rising salinity at higher pH in Fig. 2a appears incongruous. Low salt apparently engenders some adhesion even if both interfaces separately are negatively charged, if the stronger electrostatic overlap can induce coupling. The high concentration of H^+ counterions near the acid-dissociated kaolinite surfaces can protonate the oil interface, increasing its effective IEP [4]. Alternatively, polar molecules at the oil interface could reorient under the repulsion to bury their charge groups in the bulk, instead exposing polyaromatic sheets which may bind Na^+ to then be attracted to the kaolinite. On addition of even low concentrations of $CaCl_2$ in Fig. 2b, Ca^{2+} is expected to displace monovalent Na^+ counterions from both interfaces [15], in particular binding to deprotonated acid groups at the oil interface [3]. The reduction in their zeta potentials and strong screening greatly weakens electrostatic interactions and ionic contributions to adhesion at much lower salinities than are required for NaCl alone. However, in the absence of NaCl, 0.01M $CaCl_2$ actually accentuates adhesion in Fig. 2b, possibly since the kaolinite faces now resist Ca^{2+} adsorption by retaining their strongly bound H^+ counterions. In general, salinity changes in a kaolinite-rich system may shift pH [5], which can have a greater effect on oil adhesion than the salt change *per se*. In our study however, the kaolinite mass per piece is insufficient relative to brine volume in the cell to perturb the initial bulk pH.

Oil Deposition on Kaolinite from Aging

The brine/oil-treated kaolinite coats all remained intact and without any particle loss throughout the aging and cleaning procedures mentioned above. Further, if bearing a brownish tinge due to deposition, this discoloration was uniform across the piece area. The GSV, defined as ranging from 0 (completely dark) to 255 (white), was 241.0 ± 2.3 for untreated kaolinite-coated pieces. The GSV of each treated piece was subtracted from this untreated average to give a measure of the discoloration extent, termed "deposition GSV", i.e. increasing from 0 as deposition increases. For each brine, the average and standard deviation of this quantity over the 4 pieces is listed in Table 1. Deposition GSV standard deviation averages 3.7, amounting to an average coefficient of variation of 21%. Although this is quite high, due to some variability in deposition for a given brine and magnified by the subtraction of two large GSV to obtain the smaller deposition GSV, the trends are clear. These are illustrated in the 3D graphs of Figs. 2c and d, in both cases using the same format as for the corresponding contact angle results in Figs. 2a and b.

In Fig. 2c, the deposition after aging decreases with NaCl concentration for both acidic and natural pH, although far less dramatically than for contact angle hysteresis in Fig. 2a, with the most significant decrease now occurring only at the highest salinity of 1M. Further, at pH 9, deposition does not exhibit this decrease with salinity, instead giving substantial deposits at 0.1 and 1M. Thus, although the two higher pH values behave similarly for angle hysteresis, the two lower ones are more alike in deposition. While angle hysteresis decreases with pH at constant NaCl, deposition switches from decreasing to increasing with pH in Fig. 2c as salinity passes 0.1M. In short, only 3 combinations, namely 0.01M at pH 9 and 1M at pH 4 and natural, give significantly lower deposition.

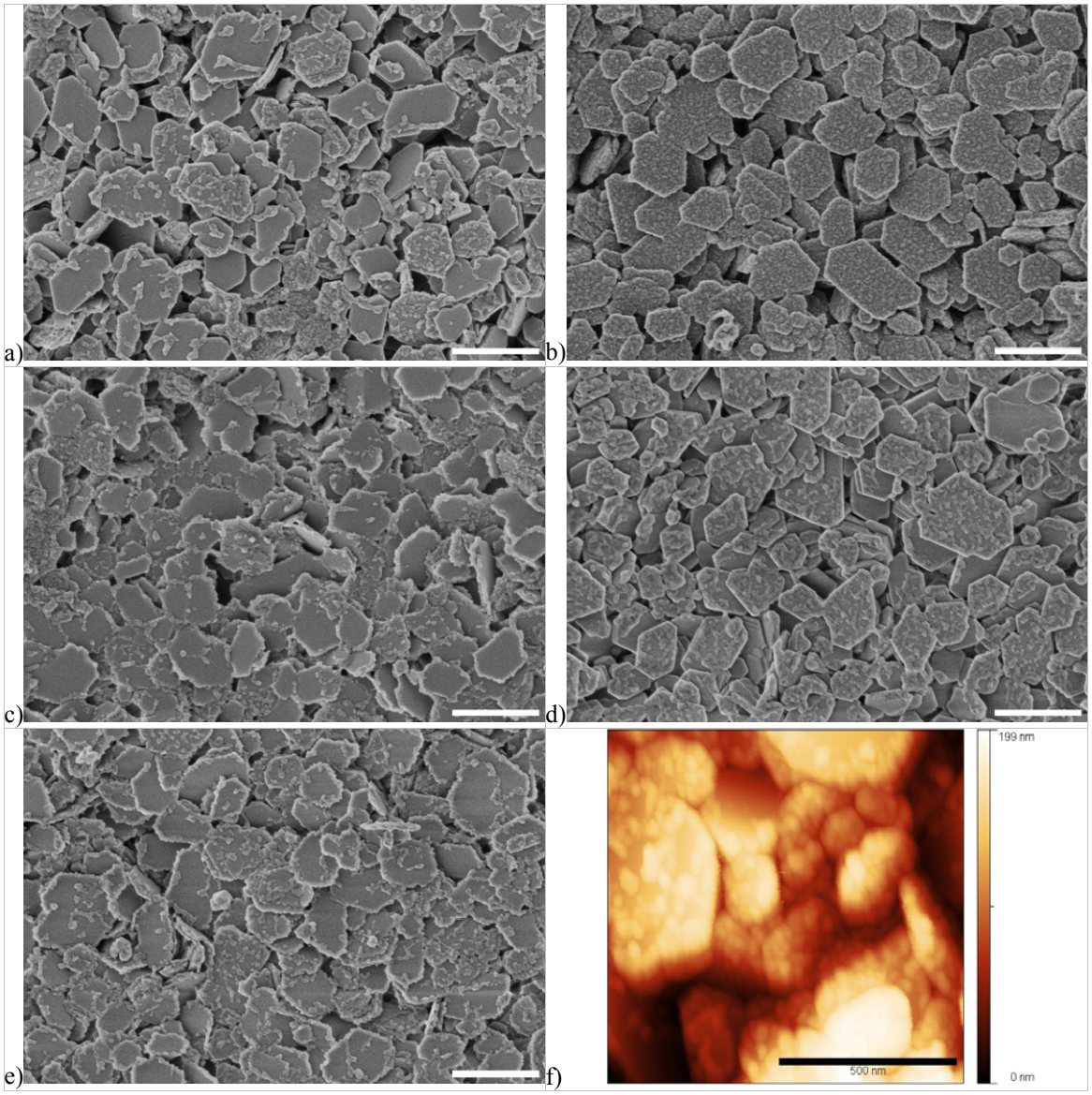

Figure 3. a-e) FESEM images, and f) AFM height image, of kaolinite-coated substrates with oil deposits after aging and flushing, for a) 0.01M NaCl at pH 9, b) 0.1M NaCl at pH n, c) 1M NaCl at pH 4, d) 0.1M NaCl + 1M $CaCl_2$ at pH n, e) 1M NaCl + 0.01M $CaCl_2$ at pH n, and f) as for b). Scale bars are 500 nm.

Figures 3a and c provide representative high-resolution SEM images of the two extremes, 0.01M at pH 9 and 1M at pH 4, respectively, while Fig. 3b is for intermediate salinity and acidity (0.1M NaCl at pH natural) with typically high deposition. For all brines, deposits take the form of primary nanoparticles, of size around 10 nm, which aggregate or merge into larger features. Further, all brines giving substantial deposition, i.e. excluding the 3 samples in Fig. 2c, appear almost identical to Fig. 3b, with a single layer of nanoparticles and their assemblies decorating all visible faces and edges of kaolinite particles. Even for kaolinite well shielded by overlying platelets providing tight constrictions, brine appears to have been displaced for oil to directly contact the surfaces and alter their wettability, as

also evidenced by the AFM image for this same system in Fig. 3f. The depth in the coat to which infiltration occurs is unknown. In Fig. 3c and the very similar images (not shown) for 1M NaCl at pH natural, kaolinite faces are relatively free from deposit, while edges are heavily covered, appearing thicker and fluffier than their sharp counterparts for untreated kaolinite in Fig. 1. Oil has again made substantial inroads into the coat surface pores, yet has been unable to deposit on faces owing to persistence of brine thin films or insufficient bonding. At the opposite compositional extreme of low salinity and high pH in Fig. 3a, the kaolinite edges are now mainly deposit-free, while outermost faces bear the majority of the sporadic deposits. For both regimes of relatively slight wettability alteration, deposit is sometimes seen to also partially span gaps between kaolinite particles, possibly due to overlap of edge deposition in the high salinity, low pH case and to the prevalence of elongated 1-D aggregates at low salinity and high pH.

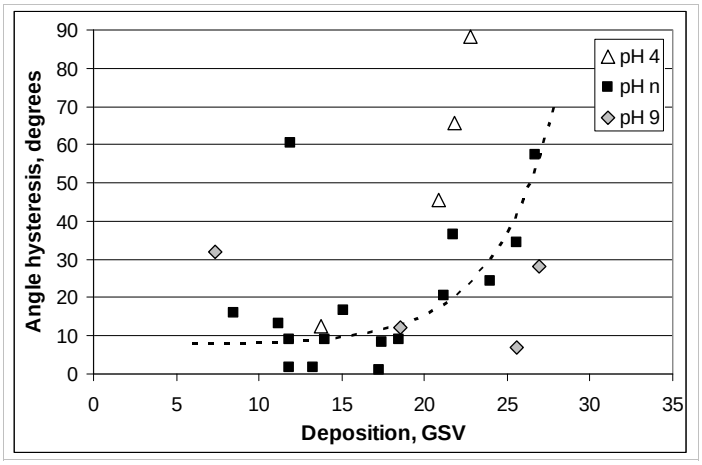

Figure 4. Plot of contact angle hysteresis versus extent of asphaltene deposition after aging, on kaolinite-coated substrates, for all brines studied at the three pH values. Dotted curve is best fit to natural pH data.

For the brines containing calcium, at natural pH, deposition in Fig. 2d lessens with Ca^{2+} content at fixed NaCl, although the trend is masked at 1M NaCl by this overwhelming presence of Na^{+}. This mirrors the trend for angle hysteresis in Fig. 2b. Both measures also generally decrease with NaCl content at fixed $CaCl_2$, although again naturally masked at high Ca^{2+}. This decrease is much clearer for angle hysteresis, due partly to deposition in the absence of NaCl being lower than expected. The scatter plot in Fig. 4 of all values in Table 1 evidences this reasonable correlation, at natural pH or at pH 4, between responses due to aging at room temperature for shorter times and at elevated temperature for longer times. For all sodium-containing brines giving substantial deposition, i.e. all but the 5 brines with 1M NaCl or $CaCl_2$ in Fig. 2d, the SEM images appear qualitatively as in Fig. 3b, bearing deposit on all faces and edges of kaolinite, both at and below the coat outer surface. Reduction in deposition GSV, e.g. from 0.01 to 0.1M $CaCl_2$ at fixed 0.1M NaCl in Fig. 2d, results from a decrease in the density of asphaltene nanoparticle coverage on each kaolinite face (not shown). It is not known whether depth of deposition below the upper realms accessible to SEM also decreases in tandem. On further increase in $CaCl_2$ content to 1M at this fixed 0.1M NaCl, the state of decreased

deposition in Fig. 2d is represented by the image in Fig. 3d. While the outer faces of the outermost particles, and their edges, bear sufficient deposit to be regarded as oil-wet, the vast majority of kaolinite below is now deposit-free, displaying clean faces and edges. The primary effect of high $CaCl_2$ concentration for this oil is thus to limit its ingress into the kaolinite aggregate. In Fig. 2e, the deposition for 1M NaCl with 0.01M $CaCl_2$ principally occurs on plate edges, as was the case for the NaCl brine without this small fraction of added Ca^{2+}, at both natural pH and pH 4 (Fig. 3c). It appears that in the high NaCl concentration regime, if $CaCl_2$ is only sparingly present and pH not too high, the main mechanism limiting oil-wetness is stabilisation of kaolinite faces against deposition.

X-ray μ-CT of Kaolinite-Rich Sandstone

The kaolinite-coated substrates were designed to render the particles immobile during contact angle measurement or aging and flushing, to avoid drop non-adhesion by coat cohesive failure or loss of deposit-bearing surface particles. Particle configuration and pore confinement is not representative of a real rock, so kaolinite in rock a) may or may not exhibit the behavior in Figs. 2-3, e.g. depending on whether its faces are accessible or it remains protected by bulk brine in an undrained throat, and b) may or may not be immobile, depending on cementation or intergrowth. A companion paper [16] addresses these fines mobilization issues in Berea sandstones. The present study considers a simpler sandstone, in which kaolinite is the dominant clay, and is more clearly imaged by μ-CT, which is the most suitable technique to quantify pore-scale movement at lengths above microns. In the single-phase experiments here, the rock plug was infiltrated with 0.1M $CaCl_2$, above the critical coagulation concentration for kaolinite [17], then flooded with 100-fold diluted brine, then with pure water. Figure 5 shows voxel-registered 2D subsets in the initial dry state and these 3 wet states. They do not reveal any significant movement of kaolinite particles in pores, even on switching to pure water, in agreement with formation damage studies [18]. Reference [16] gave a similar result, although higher resolution SEM images revealed movement of smaller kaolinite particles.

CONCLUSION

Uniform, smooth coats, of thickness ~1 μm, of fine kaolinite on glass allow extension of model substrate studies to this important component of reservoir rocks. For individual kaolinite particles separated from crude oil by only a thin brine sheath, this film is increasingly prone to rupture, to allow adhesion and deposition of oil, if the concentration of sodium and/or calcium chloride is decreased and/or brine pH is decreased. High sodium chloride salinity mainly reduces wettability alteration of kaolinite particle faces. For kaolinite aggregates, represented here by the coat, filled by brine and again shielded from oil by only a thin film, wettability alteration of outermost particle surfaces while the underlying particles remain water-wet, is more likely to occur if the calcium chloride content is high. Otherwise, oil appears capable of penetrating into the small inter-particle pores to render them oil-wet. These single-brine experiments suggest that if enhanced oil recovery via low salinity injection involves kaolinite becoming more water-wet, this is likely the result of the transient state or an indirect effect, not the true equilibrium state.

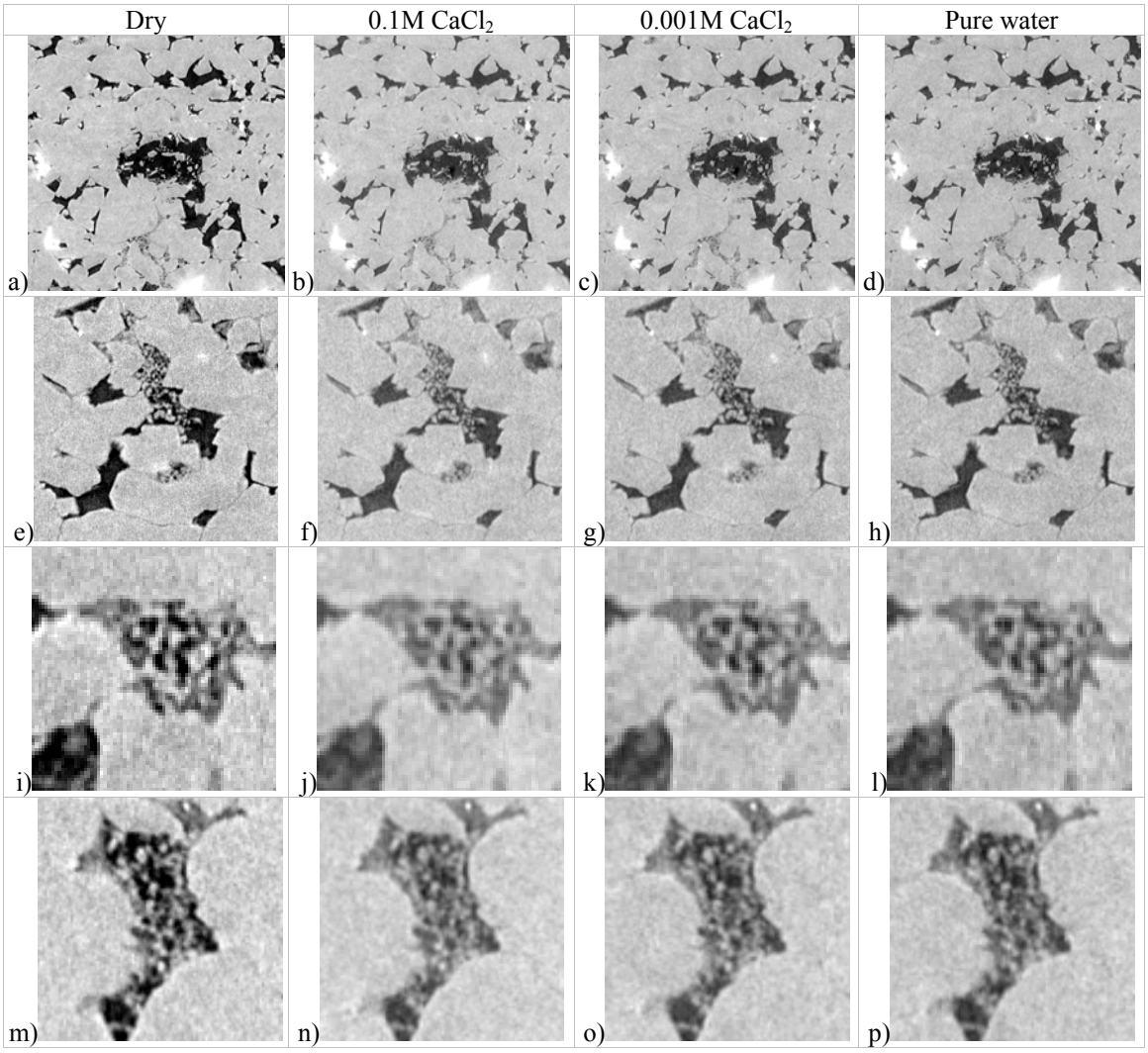

Figure 5. 2D slices of 4 registered tomograms in the dry state (column 1), and in 0.1M $CaCl_2$ (column 2), 0.001M $CaCl_2$ (column 3), and pure water (column 4) with square sub-area size: a-d) 1.896 mm , e-h) 693 μm , i-l) 225 μm, m-p) 312 μm.

ACKNOWLEDGEMENTS

The member companies of the Digital Core Consortium Wettability Satellite are thanked for support, as is the Australian Partnership for Advanced Computation for computing resources. A.F. and M.K. acknowledge support from an ARC Discovery Grant.

REFERENCES

1. Durand, C.; Rosenberg, E. “Fluid distribution in kaolinite- or illite-bearing cores: cryo-SEM observations versus bulk measurements”, *J. Pet. Sci. Eng.* (1998) **19**, 65-72.

2. Buckley, J.S.; Liu, Y.; Xie, X.; Morrow, N.R. "Asphaltenes and crude oil wetting - the effect of oil composition", *SPE J.* (1997) **2**(35366), 107-119.
3. Liu, L.; Buckley, J.S. "Alteration of wetting of mica surfaces", *J. Pet. Sci. Eng.* (1999) **24**, 75-83.
4. Buckley, J.S.; Takamura, K.; Morrow, N.R. "Influence of electrical surface charges on the wetting properties of crude oils", *SPE Res. Eng.* (1989) 332-340.
5. Tang, G.Q.; Morrow, N.R. "Influence of Brine Composition and Fines Migration on Crude Oil/Brine/Rock Interactions and Oil Recovery", *J. Pet. Sci. Eng.* (1999) **24**, 99-111.
6. Lager, A.; Webb, K.J.; Black, C.J.J.; Singleton, M.; Sorbie, K.S. "Low Salinity Oil Recovery - An Experimental Investigation", paper SCA 2006-36 presented at the 2006 SCA Internat. Symp., Trondheim, 12-16 Sept.
7. Boussour, S.; Cissokho, M.; Cordier, P.; Bertin, H.; Hamon, G. "Oil recovery by low salinity brine injection: Laboratory results outcrop and reservoir cores", SPE 124277 presented at the 2009 SPE Ann. Tech. Conf., New Orleans, 4-7 Oct.
8. Skrettingland, K.; Holt, T.; Tweheyo, M.T.; Skjevrak, I. "Snorre Low Salinity Water Injection - Core Flooding Experiments and Single Well Field Pilot", paper SPE 129877 presented at the 2010 SPE IOR Symp., Tulsa, 24-28 Apr.
9. Tie, H.G.; Tong, Z.X.; Morrow, N.R. "The effect of different crude oil/brine/rock combinations on wettability through spontaneous imbibition", paper SCA 2006-02 presented at the 2003 SCA Internat. Symp., Pau, Sept 21-24.
10. Chipera, S.J.; Bish, D.L. "Baseline studies of The Clay Minerals Society source clays: Powder x-ray diffraction analyses", *Clays Clay Miner.* (2001) **49**, 398-409.
11. Shang, J., et al. "Contact angles of aluminosilicate clays as affected by relative humidity and exchangeable cations", *Colloid Surf. A* (2010) **353**, 1-9.
12. Sakellariou, A. et al. "An x-ray tomography facility for a wide range of mesoscale physics applications", *Proceedings of SPIE* (2004) **5535**, 166-171.
13. Latham, S.; Varslot, T.; Sheppard, A. "Image registration: Enhancing and calibrating x-ray micro-CT imaging", paper SCA2008-35 presented at the 2008 SCA Symp., Abu Dhabi, 29 Oct.-2 Nov.
14. Buckley, J.S.; Morrow, N.R. "Wettability and imbibition: Microscopic distribution of wetting and its consequences at the core and field scales", Final report, US DOE contract DE-AC26-99BC15204, 2003, p.184.
15. Alkan, M.; Demirbas, O.; Dogan, M. "Electrokinetic properties of kaolinite in mono- and multivalent electrolyte solutions", *Microporous Mesoporous Mater.* (2005) **83**, 51–59.
16. Kumar, M.; Fogden, A.; Morrow, N.R.; Buckley, J.S. "Mechanisms of improved oil recovery from sandstone by low salinity flooding", paper SCA 2010-35 presented at the 2010 SCA Internat. Symp., Halifax, 4-7 Oct.
17. Goldberg, S.; Forster, H.S.; Heick, E.L. "Flocculation of illite/kaolinite and illite/montmorillonite mixtures as affected by sodium adsorption ratio and pH", *Clays Clay Miner.* (1991) **39**, 375-380.
18. Kia, S.F., Fogler, H.S., Reed, G.M., Vaidya, R.N. "Effect of salt composition on clay release in Berea sandstones", *SPE Prod. Eng.* (1987), 277-283.